Rapid Communications

Period doubling in period-one steady states

Reuben R. W. Wang,[1] Bo Xing,[1] Gabriel G. Carlo,[2] and Dario Poletti[1]

[1]*Engineering Product Development Pillar, Singapore University of Technology and Design, 8 Somapah Road, Singapore 487372, Singapore*

[2]*Departamento de Física, CNEA, Libertador 8250, (C1429BNP) Buenos Aires, Argentina*

(Received 5 September 2017; published 2 February 2018)

Nonlinear classical dissipative systems present a rich phenomenology in their "route to chaos," including period doubling, i.e., the system evolves with a period which is twice that of the driving. However, typically the attractor of a periodically driven quantum open system evolves with a period which exactly matches that of the driving. Here, we analyze a periodically driven many-body open quantum system whose classical correspondent presents period doubling. We show that by studying the dynamical correlations, it is possible to show the occurrence of period doubling in the quantum (period-one) steady state. We also discuss that such systems are natural candidates for clean and intrinsically robust Floquet time crystals.

DOI: 10.1103/PhysRevE.97.020202

I. INTRODUCTION

Classical driven and dissipative systems present a varied typology of dynamical behaviors. In these systems it is possible to observe very different types of attractors: fixed points, limit cycles, and chaotic attractors. For quantum systems, if in some limit they can be reliably described by classical equations of motion, it is also possible to observe signatures of these behaviors (see, for example, Ref. [1]).

Important types of driven dissipative systems are those for which the driving is time periodic. The steady state of such systems, when unique, has a periodicity which is given exactly by the period of the driving, even if the classical corresponding system presents period doubling or is chaotic [2]. Hence these systems deserve further investigations.

An important insight into quantum systems is given by two-time correlations. For instance, current-current correlations on a thermal state can be used to infer its linear response transport properties. For the case of quantum steady states, it was shown that the two-time correlations of a dissipative engineered quantum state can be significantly different from those of the target state [3].

Here, we show that by analyzing the two-time correlations of periodic steady states, with a period exactly given by the driving period, it is possible to observe a period doubling in the evolution of the correlation. This occurs when the corresponding classical system is in a parameter regime for which period doubling occurs and when the effective Planck constant is small enough that the quantum dynamics mimics the classical dynamics for long enough times. The presence of an underlying period doubling classical dynamics also naturally allows one to interpret these systems as a clean Floquet time crystal [4–9]. Moreover, the two-time correlation analysis of the periodic steady state allows one to characterize it as an intrinsically robust Floquet time crystal.

This Rapid Communication is divided as follows: In Sec. II we introduce the model, then we describe its bifurcation map in Sec. III, analyze the spectrum of the periodic propagator in Sec. IV, and show the presence of period doubling in the steady state in Sec. V. In Sec. VI we discuss that the system is a natural example of a clean Floquet time crystal, and finally in Sec. VII we draw our conclusions.

II. MODEL, PERIODIC STEADY STATE, AND MEAN-FIELD EQUATIONS

We consider a double-well potential with N atoms which is periodically driven and under the influence of dissipation. The system is described by a master equation whose time-dependent generator $\mathcal{L}_t$, of Lindblad form [10–13], is composed of two parts,

$$\dot{\hat{\rho}} = \mathcal{L}_t(\hat{\rho}) = -i[\hat{H}(t), \hat{\rho}] + \mathcal{D}(\hat{\rho}). \tag{1}$$

Note that we have set $\hbar = 1$. The first part of Eq. (1) describes the Hamiltonian evolution of the system's density operator $\hat{\rho}$, due to the Hamiltonian $\hat{H}(t)$. We consider a double well whose Hamiltonian is

$$\hat{H}(t) = -J(\hat{b}_1^\dagger \hat{b}_2 + \hat{b}_2^\dagger \hat{b}_1) + \frac{U}{2} \sum_{j=1,2} \hat{n}_j(\hat{n}_j - 1) + \varepsilon(t)(\hat{n}_2 - \hat{n}_1), \tag{2}$$

where $\hat{b}_j$ ($\hat{b}_j^\dagger$) annihilates (creates) a boson at site j, while $\hat{n}_j = \hat{b}_j^\dagger \hat{b}_j$. The Hamiltonian parameters are J, the tunneling amplitude, U, the interaction strength, and $\varepsilon(t)$, the modulation of the local potential. The modulation $\varepsilon(t)$ is chosen to be periodic of period $T = 2\pi/\omega$, i.e., $\varepsilon(t) = \varepsilon(t+T) = \mu_0 + \mu_1 \sin(\omega t)$, where μ_0 and μ_1 are, respectively, a static and a dynamic energy offset between the two sites. This double-well Hamiltonian has been investigated in both theoretical [14–17] and experimental [18,19] works.

The second part of $\mathcal{L}_t$ in Eq. (1) describes the dissipative evolution due to the dissipator,

$$\mathcal{D}(\hat{\rho}) = \gamma(2\hat{\Gamma}\hat{\rho}\hat{\Gamma}^\dagger - \{\hat{\Gamma}^\dagger\hat{\Gamma}, \hat{\rho}\}), \tag{3}$$

where γ is the dissipative rate while the jump operator is given by [20–23]

$$\hat{\Gamma} = (\hat{b}_1^\dagger + \hat{b}_2^\dagger)(\hat{b}_1 - \hat{b}_2). \tag{4}$$

This model has been investigated in Refs. [2,24].

It was shown in detail in Ref. [2] that, given the periodicity of $\mathcal{L}_t$, it is possible to generate a Floquet map $\mathcal{P}_F = \mathcal{P}_{0,T}$, where $\mathcal{P}_{t_1,t_2} = \mathcal{T} e^{\int_{t_1}^{t_2} \mathcal{L}_t d\tau}$ and $\mathcal{T}$ is the time-ordering operator. The fixed point of this map is the periodic steady state of the system $\hat{\rho}_s(mT)$, where m is an integer number [25]. To compute $\hat{\rho}_s(t)$ at times $t \neq mT$, it is sufficient to evolve $\hat{\rho}(0)$ from time 0 to t using Eq. (1).

An important insight into the dynamics of this system is obtained, especially for a large number of particles, by studying the corresponding classical mean-field equations of motion. To compute them, it is convenient to first rewrite Eq. (1) in terms of the spin operators $\hat{S}_x = \frac{1}{2N}(\hat{b}_1^\dagger \hat{b}_2 + \hat{b}_2^\dagger \hat{b}_1)$, $\hat{S}_y = -\frac{i}{2N}(\hat{b}_1^\dagger \hat{b}_2 - \hat{b}_2^\dagger \hat{b}_1)$, and $\hat{S}_z = \frac{1}{2N}(\hat{n}_1 - \hat{n}_2)$, and study their evolution in the Heisenberg picture [13]. The commutator between these operators is $[\hat{S}_x, \hat{S}_y] = i\frac{\hat{S}_z}{N}$ and cyclic permutations. This implies that as $N \to \infty$, these spin operators commute, resulting in classical equations of motion (see Ref. [2] for more details).

Since $\langle \hat{S}^2 \rangle = \langle \hat{S}_z^2 \rangle + \langle \hat{S}_x^2 \rangle + \langle \hat{S}_y^2 \rangle$ is a constant of motion (we have used the notation $\langle \hat{O} \rangle = \mathrm{tr}\,[\hat{\rho}\hat{O}]$ for the expectation value of the operator $\hat{O}$), it is possible to write the mean-field equations of motion of the system in terms of two angle variables θ and ϕ defined by $(\langle S_x \rangle, \langle S_y \rangle, \langle S_z \rangle) = \frac{1}{2}[\cos(\varphi)\sin(\vartheta), \sin(\varphi)\sin(\vartheta), \cos(\vartheta)]$. We thus get the equations of motion [2],

$$\dot{\vartheta} = 2J\sin(\varphi) + 4\gamma N \cos(\varphi)\cos(\vartheta)$$
$$\dot{\varphi} = 2J\frac{\cos(\vartheta)}{\sin(\vartheta)}\cos(\varphi) - 2\varepsilon(t) + UN\cos(\vartheta) - 4\gamma N \frac{\sin(\varphi)}{\sin(\vartheta)}. \quad (5)$$

III. BIFURCATION MAP

For a more complete and self-contained analysis, we now study the quantum and classical bifurcation map for this system in Fig. 1 [26]. More precisely, for the classical map we evolve Eq. (5) for different initial conditions uniformly distributed over $\vartheta \in [-\pi, \pi]$ and $\phi \in [0, 2\pi]$ for $t = 800T$. We then record stroboscopically at times which are integer multiples of the driving period, $t = mT$, the value of ϑ [and hence of $\langle \hat{S}^z \rangle = 1/2\cos(\vartheta)$] for the next 200 (or more) periods and represent them in Fig. 1(a). For a different interacting model [27], a quantum bifurcation map was produced using the trajectory method for the evolution of the density matrix [28]. In Figs. 1(b) and 1(c) we show the quantum bifurcation map from another approach. For any given value of the interaction we compute the steady state $\hat{\rho}_s(0)$ and then we project it over the eigenstates of $\hat{S}^z$ and take the trace. More precisely, we can write $\hat{S}^z = \sum_n \hat{S}_n^z$, where $\hat{S}_n^z = (n/N - 1/2)|n, N-n\rangle\langle n, N-n|$ and the state $|n, N-n\rangle$ has n particles in site 1 and $N-n$ in site 2. We thus compute $\langle \hat{S}_n^z \rangle_s = \mathrm{tr}\,[\hat{S}_n^z \hat{\rho}_s(0)]$ and produce an intensity plot as a function of both $\langle \hat{S}_n^z \rangle_s$ and the interaction strength U/J. We have used the notation $\langle \cdots \rangle_s$ to remind the reader that the trace is taken over the steady state. In Figs. 1(b) and 1(c) we show the bifurcation map respectively for $N = 25$ and $N = 100$ atoms. For the larger number of particles it is possible to see more clearly the underlying structure related to the mean-field classical corresponding equations.

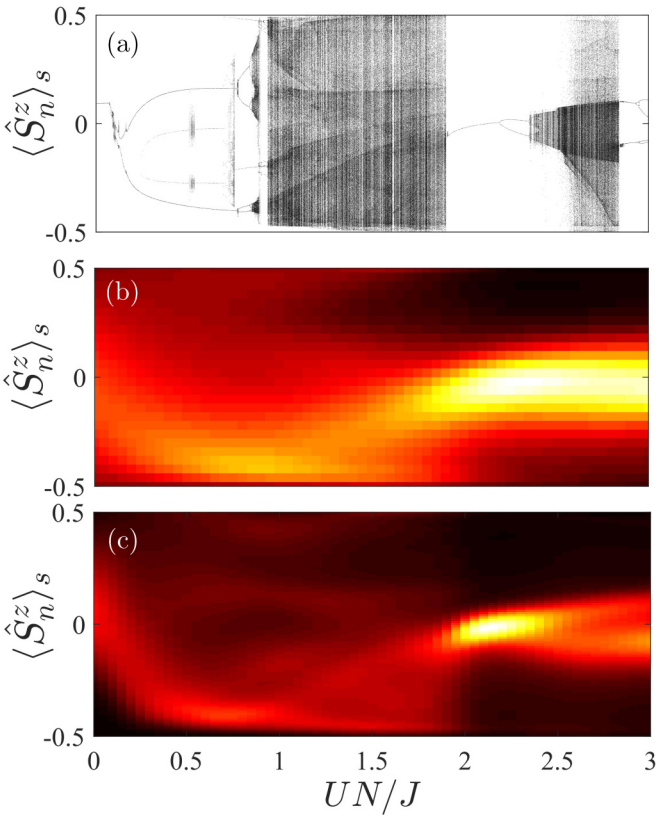

FIG. 1. Bifurcation maps for (a) classical mean-field equations (5), and (b), (c) a quantum system with respectively $N = 25$ and $N = 100$. The other parameters are $\mu_0 = J$, $\mu_1 = 3.4J$, and $\gamma N = 0.1J$.

IV. SPECTRUM OF THE FLOQUET MAP

A signature of the presence of a bifurcation in the classical corresponding system leaves signatures in the spectrum of the Floquet map $\mathcal{P}_F$. We thus compute the eigenvalues of $\mathcal{P}_F$, which we refer to as "Floquet rapidities" λ_j [29], for different particle numbers and we plot them in a complex plane in Fig. 2. In particular, Figs. 2(a)–2(d) correspond respectively to $N =$ 10, 25, 50, and 100. Since the periodic steady state is unique, one Floquet rapidity has exactly the value 1. We note that as the number of particles increases, there is a Floquet rapidity which approaches, but does not reach, the value -1 on the real axis (we highlight this point in red). The presence of such a slow decaying state with Floquet rapidity ≈ -1 indicates that dynamical properties can show an oscillatory behavior with a period which is twice that of the driving.

V. TWO-TIME CORRELATIONS AND PERIOD DOUBLING

As stated before, the steady state is the fixed point of the map $\mathcal{P}_F$, which implies that $\hat{\rho}_s(mT) = \hat{\rho}_s(0)$ for any integer m. As a consequence, any static (i.e., single time) observable computed on the steady state is exactly periodic with the period of the steady state. More precisely, given an operator $\hat{O}$, we have that

$$\langle \hat{O}(mT) \rangle_s = \mathrm{tr}[\hat{O}\rho_s(mT)] = \mathrm{tr}[\hat{O}\rho_s(m'T)] = \langle \hat{O}(m'T) \rangle_s, \quad (6)$$

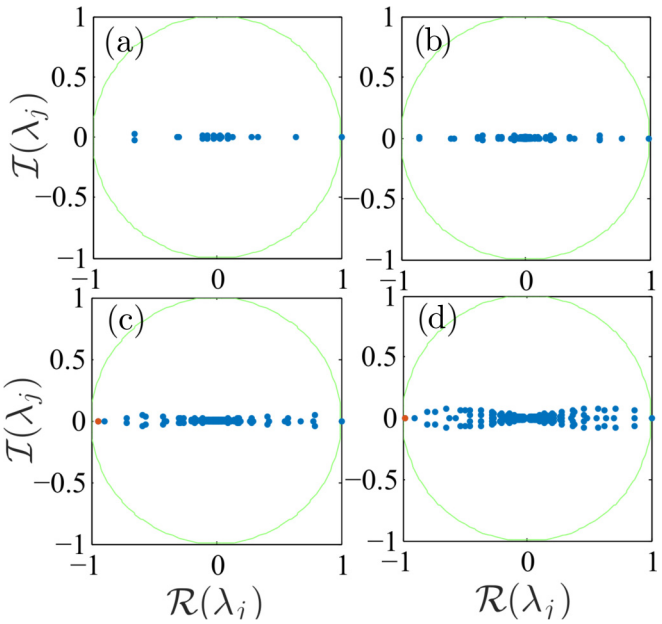

FIG. 2. Real and imaginary parts of the spectrum of the Floquet rapidities for (a) $N = 10$, (b) $N = 25$, (c) $N = 50$, and (d) $N = 100$. The red dots in (c) and (d) represent the slowest decaying state. The other parameters are $\mu_0 = J$, $\mu_1 = 3.4J$, $UN = 0.2J$, and $\gamma N = 0.1J$.

with $m' \neq m$. It is very important to stress that this result is independent of the underlying dynamics of the classical corresponding system, and whether the classical attractor is regular, with or without bifurcation, or chaotic.

In Sec. III we have also shown the quantum and classical corresponding bifurcation map of this system. This shows that at each period there is a multimodal probability distribution for the distribution of particles between the two wells. However, since this is a static observable of the steady state, it exactly repeats itself at each period, i.e., this is not evidence of period doubling.

In order to reveal the presence of period doubling, we need instead to study dynamic correlations on the steady state. In particular, we study the two-time correlation,

$$\langle \hat{S}^z(mT)\hat{S}^z(0)\rangle_s = \mathrm{tr}[\hat{S}^z(\mathcal{P}_F)^m \hat{S}^z \hat{\rho}_s(0)]. \quad (7)$$

We plot $\langle \hat{S}^z(mT)\hat{S}^z(0)\rangle_s$ in Fig. 3 as a function of time for different total particle numbers N. Figure 3 demonstrates that the two-time correlation evolves with a period which is twice that of the driving T for an amount of time which becomes longer the more atoms are in the system [30]. From our previous analysis of the Floquet rapidities, we can understand this behavior from the presence of a Floquet rapidity close to -1. Once the operator $\hat{S}^z$ acts on the steady state, we can write the resulting operator as a superposition of $\hat{\rho}_j$, the eigenoperators of the Floquet propagator $\mathcal{P}_F$, with eigenvalues (Floquet rapidities) λ_j, i.e., $\hat{S}^z\hat{\rho}_s(0) = \sum_j c_j \hat{\rho}_j$, where the c_j are scalars. From this it is easy to show that the (stroboscopic) time evolution of such an operator is given by

$$\mathcal{P}_{0,mT}[\hat{S}^z\hat{\rho}_s(0)] = \sum_j c_j \hat{\rho}_j \lambda_j^m. \quad (8)$$

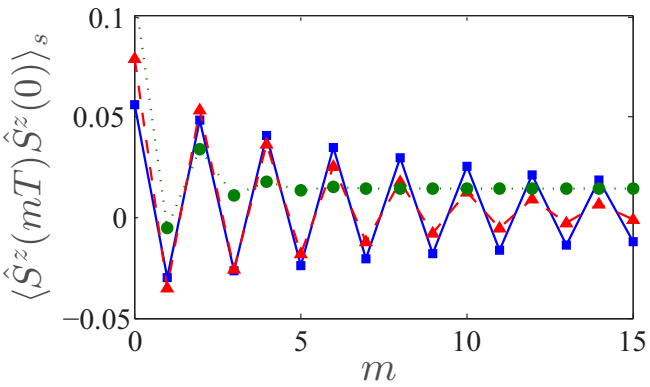

FIG. 3. Two-time correlation $\langle \hat{S}^z(nT)\hat{S}^z(0)\rangle_s$ vs time for a total particle number $N = 5$ (green circles), $N = 25$ (red triangles), and $N = 100$ (blue squares). Other parameters are $UN = 0.2J$, $\mu_0 = J$, $\mu_1 = 3.4J$, and $\gamma N = 0.1J$.

As shown in Fig. 2, for parameters such that the classical corresponding dynamics has bifurcation, and for a large enough particle number, the spectrum of $\mathcal{P}_F$ has, on top of the steady state, another eigenvalue close to the unit circle which is positioned close to the value -1. The periodic steady state operator $\hat{\rho}_s$ and the one corresponding to eigenvalue -1, i.e., $\hat{\rho}_{-1}$, will dominate the long-time dynamics [31],

$$\mathcal{P}_{0,mT}[\hat{S}^z\hat{\rho}_s(0)] \approx c_s\hat{\rho}_s + c_{-1}\hat{\rho}_{-1}(-1)^m. \quad (9)$$

The second term on the right-hand side of Eq. (9) is the one responsible of the period-two evolution of the two-time correlation function $\langle \hat{S}^z(mT)\hat{S}^z(0)\rangle_s$. In fact, this correlation, at long enough times, can be approximated by

$$\langle \hat{S}^z(mT)\hat{S}^z(0)\rangle_s \approx c_s\,\mathrm{tr}(\hat{S}^z\hat{\rho}_s) + c_{-1}\,\mathrm{tr}(\hat{S}^z\hat{\rho}_{-1})(-1)^m, \quad (10)$$

which oscillates with a period $2T$, i.e., twice that of the driving.

The presence of an underlying classical period doubling dynamics carries other interesting consequences. It has been shown before that for a system in which both the Hamiltonian and the dissipator are number conserving, two-time correlators of the type $\langle \hat{A}(t)\hat{B}(0)\rangle$ behave very differently depending on whether or not the first operator included in the two-time correlator $\hat{B}$ is number conserving [3,32]. When the first operator is number conserving, it is possible to observe very slow dynamics such as power-law decays, stretched exponentials, and aging [3,17,33]. However, when the first operator is not number conserving, the dynamics is bound to be an overall exponential decay [3]. We then analyze the two-time correlator $\langle \hat{b}_2^\dagger(t)\hat{b}_1(0)\rangle$ in which each operator does not conserve the total particle number and for which exponential decay is expected.

In Fig. 4 we depict $|\langle \hat{b}_2^\dagger(mT)\hat{b}_1(0)\rangle|$ versus the number of periods m. In particular, we show in Figs. 4(a) and 4(b) the case for which the corresponding classical dynamics has period doubling, $UN = 0.2J$, while for the parameters of Figs. 4(c) and 4(d), the classical mean-field equations predict chaotic motion, $UN = 1.6J$. Figure 4(a) clearly shows signatures of period doubling and also that the decay time scale increases with the number of particles N. At the same time, the relaxation is still exponential, as evidenced by the log-lin plot in Fig. 4(b). In Figs. 4(c) and 4(d), for which the corresponding classical

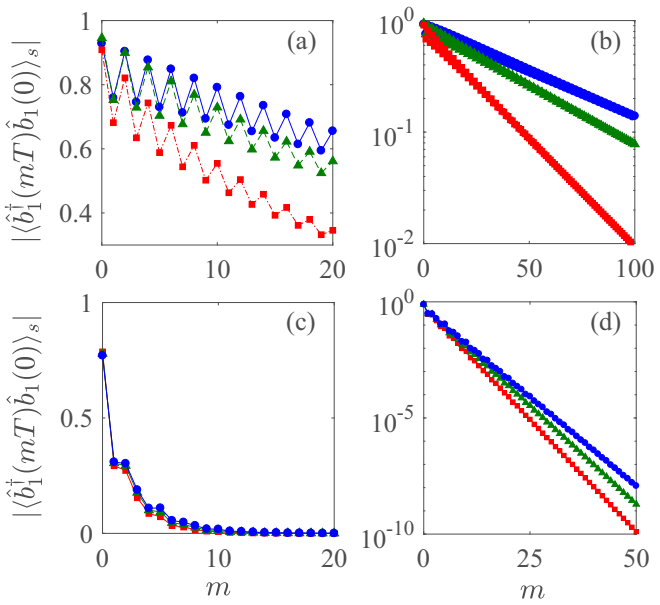

FIG. 4. Absolute value of the two-time correlator $\langle \hat{b}_2^\dagger(t)\hat{b}_1(0)\rangle$ vs number of periods m for different particle numbers $N = 25$ (red squares with dotted-dashed line), $N = 50$ (green triangle with dashed line), and $N = 100$ (blue circles with continuous line). In (a) and (b) we show the case near a period doubling, $UN = 0.2J$, respectively, in a lin-lin and in a log-lin plot. In (c) and (d) we show the case of a chaotic region, $UN = 1.6J$, respectively, in lin-lin and in log-lin. Other parameters are $\mu_0 = J$, $\mu_1 = 3.4J$, and $\gamma N = 0.1J$.

equations are chaotic, we observe a much more rapid exponential decay, and no signatures of period doubling. This analysis highlights that for large N not only is period doubling present for number conserving operators, but also for non-number conserving operators. The presence of a classical limit with period doubling makes the dynamics particularly robust.

VI. BIFURCATION AS DRIVER OF CLEAN FLOQUET TIME CRYSTALS

Clean Floquet time crystals are defined as systems which in the thermodynamic limit fulfill the following properties: (i) There is a quantity which does not evolve with the period of the driving; (ii) it presents a periodic evolution without fine tuning of the system parameters; and (iii) the periodic evolution should persist for an indefinitely long time [6]. If a quantum open periodically driven system has a classical correspondent which is in a period-doubling regime, then it is straightforward to show that there are initial conditions which are robust both to changes in their exact position and of the system parameters, and which show an evolution with a period different from the driving in the thermodynamic limit. To show this, we take a coherent state centered in one of the two periodic points of the classical Poincaré section from Eq. (5) and we evolve it in time. The coherent state is given by [34]

$$|\phi(\vartheta,\varphi)\rangle = \sum_{n=0}^{N} f_n(\vartheta,\varphi)|n, N-n\rangle, \tag{11}$$

where $f_n = \sqrt{\binom{N}{n}}[\cos(\frac{\vartheta}{2})]^n[\sin(\frac{\vartheta}{2})e^{i\phi}]^{N-n}$. In Figs. 5(a)–5(f) we show stroboscopic images of the state as it evolves in time. Each panel is a Poincaré-Husimi section obtained by projecting the evolving state over coherent states. In particular, we show the Poincaré-Husimi section of the state for times $t = 0$, T, $2T$, $6T$, $7T$, and $8T$. We can observe that the coherent state jumps between two different positions, which is the expected behavior for classical period doubling. Due to the finite number of particles, we also observe a broadening of the state. In Figs. 5(g) and 5(h) we focus on the stability of this dynamics. In Fig. 5(g) we show the evolution of $\langle \hat{S}^z \rangle$ versus time for different initial conditions close to one of the classical periodic points. In Fig. 5(h) instead we vary the system parameters, still within the region of classical period doubling, and we observe that the evolution is stable. As expected, the dynamics of this

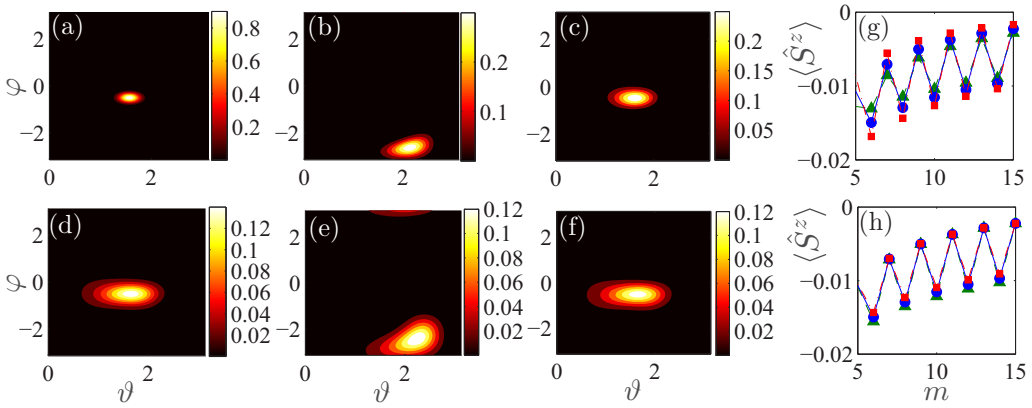

FIG. 5. (a)–(f) Poincaré-Husimi section of the evolution of a coherent state centered at one of the two classical periodic points of the classical Poincaré map. In particular, the times are (a) $t = 0$, (b) $t = T$, (c) $t = 2T$, (d) $t = 6T$, (e) $t = 7T$, and (f) $t = 8T$. (g) and (h) show $\langle \hat{S}^z \rangle$ at times given by different integers of period $t = mT$. In (g) we show that the evolution shows an alternating evolution for different initial conditions. In particular, we chose coherent states centered in the points $(\vartheta,\varphi) = (2,-3)$ (blue circles), $(1.95,-3.05)$ (green triangles), and $(2.05,-2.95)$ (red squares). The strength of the interaction in (a)–(g) is $UN = 0.2J$. In (h) we show the robustness of the motion to different system parameters. In particular, we evolve a coherent state centered at $(\vartheta,\varphi) = (2,-3)$ for parameters $UN = 0.2J$ (blue circles), $UN = 0.21J$ (green triangles), and $UN = 0.19J$ (red squares). Common parameters in (a)–(h) are $\mu_0 = J$, $\mu_1 = 3.4J$, $\gamma N = 0.1J$.

system fulfills the properties of a clean Floquet time crystal [6]. However, it should be stressed here that, while such a time crystal is robust against small changes of the parameters and of the initial condition, it is not completely robust to the initial condition. Instead, the steady state of the system is a perfect example of a robust Floquet time crystal because it is completely independent of the initial condition. We build upon Ref. [35], where the authors defined a time crystal as having long-range crystalline order in two-time correlations (it is by this starting point that they proved the nonexistence of quantum time crystals in equilibrium systems). Since the two-time correlator on the steady state can manifest period doubling, as shown in Fig. 3, the steady state is a Floquet time crystal which, given an atom number N, is completely independent of the initial condition.

Recently, we became aware of a partially related article [8], which discusses the connection between Floquet time crystals and bifurcations. However, this work does not study the dynamical correlations of the system which are necessary to establish the steady state as an intrinsically robust Floquet time crystal.

VII. CONCLUSIONS

In periodically driven open quantum systems the density operator of the steady state typically evolves with a period which exactly matches that of the driving. This implies that static observables measured on these steady states can also oscillate at the same period, but not at multiples of it. Here, we have presented clear signatures of period doubling in such steady states when studying their dynamical correlations, and we have shown that the period doubling is due to the dynamics of the underlying classical correspondent system. The occurrence of period doubling can be predicted by the presence of a Floquet rapidity which approaches -1 and can induce oscillations of period $2T$ in dynamic observables. We have also shown that this open many-body quantum system can behave as a clean Floquet time crystal. Moreover, characterizing a time crystal as having long-range order in time [35], the (period-one) steady state emerges as a Floquet time crystal which is completely robust to initial conditions.

Future works could study the complete route to chaos in periodically driven many-body open quantum systems. Another emerging important future direction is that of a many-body periodically driven open system in the presence of disorder [36,37], and, in particular, of how disorder affects the dynamics here studied.

ACKNOWLEDGMENTS

This work was supported by the Air Force Office of Scientific Research under Award No. FA2386-16-1-4041. D.P. acknowledges discussions with S. Denisov, R. Fazio, M. Hartmann, A. Rosch, and A. Russomanno.

R.R.W.W. and B.X. contributed equally to this work.

[1] P. Cvitanovic, R. Artuso, R. Mainieri, G. Tanner, and G. Vattay, *Chaos: Classical and Quantum* (Niels Bohr Institute, Copenhagen, 2014), chaosbook.org.

[2] M. Hartmann, D. Poletti, M. Ivanchenko, S. Denisov, and P. Hänggi, New J. Phys. **19**, 083011 (2017).

[3] B. Sciolla, D. Poletti, and C. Kollath, Phys. Rev. Lett. **114**, 170401 (2015).

[4] K. Sacha and J. Zakrzewski, Rep. Prog. Phys. **81**, 016401 (2018).

[5] K. Sacha, Phys. Rev. A **91**, 033617 (2015).

[6] B. Huang, Y.-H. Wu, and. W. V. Liu, arXiv:1703.04663.

[7] A. Russomanno, F. Iemini, M. Dalmonte, and R. Fazio, Phys. Rev. B **95**, 214307 (2017).

[8] Z. Gong, R. Hamazaki, and M. Ueda, arXiv:1708.01472.

[9] F. Iemini, A. Russomanno, J. Keeling, M. Schirò, M. Dalmonte, and R. Fazio, arXiv:1708.05014.

[10] G. Lindblad, Commun. Math. Phys. **48**, 119 (1976).

[11] V. Gorini, A. Kossakowski, and E. C. G. Sudarshan, J. Math. Phys. **17**, 821 (1976).

[12] R. Alicki and K. Lendi, *Quantum Dynamical Semigroups and Applications*, Lecture Notes in Physics Vol. 286 (Springer, Berlin, 1987).

[13] H.-P. Breuer and F. Petruccione, *The Theory of Open Quantum Systems* (Oxford University Press, Oxford, U.K., 2002).

[14] C. Weiss and N. Teichmann, Phys. Rev. Lett. **100**, 140408 (2008).

[15] A. Vardi and J. R. Anglin, Phys. Rev. Lett. **86**, 568 (2001).

[16] F. Trimborn, D. Witthaut, and S. Wimberger, J. Phys. B: At. Mol. Opt. Phys. **41**, 171001 (2008).

[17] D. Poletti, J.-S. Bernier, A. Georges, and C. Kollath, Phys. Rev. Lett. **109**, 045302 (2012).

[18] C. Gross, T. Zibold, E. Nicklas, J. Esteve, and M. K. Oberthaler, Nature (London) **464**, 1165 (2010).

[19] J. Tomkovič, W. Muessel, H. Strobel, S. Löck, P. Schlagheck, R. Ketzmerick, and M. K. Oberthaler, Phys. Rev. A **95**, 011602(R) (2017).

[20] S. Diehl, A. Micheli, A. Kantian, B. Kraus, H. P. Büchler, and P. Zoller, Nat. Phys. **4**, 878 (2008).

[21] S. Diehl, A. Tomadin, A. Micheli, R. Fazio, and P. Zoller, Phys. Rev. Lett. **105**, 015702 (2010).

[22] In general, the periodic driving also affects the coupling of the system to the environment. However, here we consider the case in which this effect has been compensated to give some time-independent jump operators. We stress that our results are general and not dependent on the particular evolution of the quantum open system, as long as the classical limit gives a rich dynamics with period doubling and a route to chaos.

[23] A too fast driving would imply that the time scale of the system could be faster than the relaxation time scale of the bath. We thus use a slow driving $\omega = J$, which still allows us to reveal the period doubling.

[24] V. Volokitin, A. Liniov, I. Meyerov, M. Hartmann, M. Ivanchenko, P. Hänggi, and S. Denisov, Phys. Rev. E **96**, 053313 (2017).

[25] In our case, the steady state is unique.

[26] The bifurcation map from the mean-field equations (5) has been previously discussed in Ref. [2].

[27] M. Ivanchenko, E. Kozinov, V. Volokitin, A. Liniov, I. Meyerov, and S. Denisov, Ann. Phys. **529**, 1600402 (2017).
[28] J. Dalibard, Y. Castin, and K. Mølmer, Phys. Rev. Lett. **68**, 580 (1992).
[29] T. Prosen, New J. Phys. **10**, 043026 (2008).
[30] The infinite time asymptotic value of the two-time correlation is given by $\langle \hat{S}^z \rangle_s^2$, and it can be tuned by varying the system parameters.
[31] This is true, provided, as in our case, that there is a spectral gap between the eigenvalue close to -1 and the next one closer to the unit circle.
[32] C. Guo and D. Poletti, Phys. Rev. B **96**, 165409 (2017).
[33] D. Poletti, P. Barmettler, A. Georges, and C. Kollath, Phys. Rev. Lett. **111**, 195301 (2013).
[34] F. T. Arecchi, E. Courtens, R. Gilmore, and H. Thomas, Phys. Rev. A **6**, 2211 (1972).
[35] H. Watanabe and M. Oshikawa, Phys. Rev. Lett. **114**, 251603 (2015).
[36] X. Xu, C. Guo, and D. Poletti, arXiv:1709.08934.
[37] I. Vakulchyk, I. Yusipov, M. Ivanchenko, S. Flach, and S. Denisov, arXiv:1709.08882.